BIOCHEMISTRY
including biophysical chemistry & molecular biology

Article

The roles of small laccases from Streptomyces in lignin degradation

Sudipta Majumdar, Tiit Lukk, Jose O. Solbiati, Stefan Bauer, Satish K Nair, John E. Cronan, and John A. Gerlt

Biochemistry, **Just Accepted Manuscript** • DOI: 10.1021/bi500285t • Publication Date (Web): 28 May 2014

Biochemistry is published by the American Chemical Society. 1155 Sixteenth Street N.W., Washington, DC 20036

The roles of small laccases from *Streptomyces* in lignin degradation

Sudipta Majumdar[‡,#,*], Tiit Lukk[‡,¥], Jose O. Solbiati[‡], Stefan Bauer[±], Satish K. Nair[‡], John E. Cronan[‡], and John A. Gerlt[‡]

[‡]*Institute for Genomic Biology, University of Illinois at Urbana-Champaign, Illinois 61801 and*

[±]*Energy Biosciences Institute, University of California, Berkeley, California 94720*

[#]Current address: Columbia University, New York City, New York 10027, [¥]Cornell University, Ithaca, New York 14853

[*]To whom correspondence should be addressed: Sudipta Majumdar, Department of Chemical Engineering, Columbia University; telephone, (212) 854-1444; email, sm3577@columbia.edu

Funding information:

This research was supported by Energy Biosciences Institute, University of Illinois at Urbana-Champaign, Illinois 61801. Use of the Advanced Photon Source was supported by the U.S. Department of Energy, Office of Sciences, under Contact No. DE-AC02-06CH11357; LS-CAT Sector 21 is supported by the Michigan Economic Development Corporation and the Michigan Technology Tri-Corridor (Grant 085P1000817).

The authors declare no competing financial interest.

ABBREVIATIONS

LiP, lignin peroxidase; MnP, manganese peroxidase; SCLAC, *Streptomyces coelicolor* laccase; SLLAC, *Streptomyces lividans* laccase; SVLAC, *Streptomyces viridosporus* laccase; AMLAC, *Amycolatopsis* laccase; TAT, twin-arginine translocation; LM-OMe, 1-(3,4-dimethoxyphenyl)-2-(2-methoxyphenoxy)-1,3-dihydroxypropane; LM-OH, 1-(3-methoxy-4-hydroxy)-2-(2-methoxyphenoxy)-1,3-dihydroxypropane; ABTS, 2,2'-azino-bis(3-ethylbenzothiazoline-6-sulfonate); DMP, 2,6-dimethoxy phenol; AV, acetovanillone; HOBt, hydroxybenzotiazole; CH_3CN, acetonitrile; DMSO, dimethyl sulfoxide; $MgCl_2$, magnesium chloride; NaCl, sodium chloride; HCl, hydrochloric acid; KCl, potassium chloride; Na_2HPO_4, disodium hydrogen phosphate; KH_2PO_4, potassium dihydrogen phosphate; $CuSO_4$, copper sulfate; DMF, dimethyl formamide; PBS, phosphate buffered saline; dNTP, deoxyribinucleotide; DNA, deoxyribonucleic acid; FAD, flavin adenine dinucleotide; LB, luria-bertani; IPTG, isopropyl β-D-1 thipgalactopyranoside; 3-HAA, 3-hydroxyanthranilic acid; OD, optical density; HPLC, high-performance liquid chromatography; LCMS-IT-TOF, liquid chromatography mass spectrometry ion-trap time-of-flight; PCR, polymerase chain reaction; UV-Vis, ultraviolet-visible; k_{rel}, relative rate constant; K_{app}, apparent K_M.

ABSTRACT: Laccases (EC 1.10.3.2) are multicopper oxidases able to oxidize a range of substrates including phenols, aromatic amines and non-phenolic substrates. In order to investigate the involvement of the small *Streptomyces* laccases in lignin degradation, we generated acid-precipitable polymeric lignin (APPL) obtained in the presence of wild type *Streptomyces coelicolor* A3(2) (SCWT) and its laccase-less mutant (SCΔLAC) in presence of *Miscanthus x giganteus* lignocellulose. The results showed that strain SCΔLAC was inefficient in degrading lignin compared to strain SCWT, thereby supporting the importance of laccase for lignin degradation by *Streptomyces coelicolor* A3(2). We also studied the lignin degradation activity of laccases from *Streptomyces coelicolor* A3(2), *Streptomyces lividans* TK24, *Streptomyces viridosporus* T7A and *Amycolatopsis sp.* 75iv2 using both lignin model compounds and ethanosolv lignin. All four laccases degraded a phenolic model compound (LM-OH), but only able to oxidize a non-phenolic model compound (LM-OMe) in the presence of redox mediators. Their activities are highest at pH 8.0 with a low k_{rel}/K_{app} for LM-OH, suggesting that the enzymes' natural substrates must be different in shape or chemical nature. Crystal structures of the laccases from *Streptomyces viridosporus* T7A (SVLAC) and *Amycolatopsis sp.* 75iv2 (AMLAC) were determined both with and without bound substrate. This is the first report of a crystal structure for any laccase bound to a non-phenolic *β-O-4* lignin model compound. An additional zinc metal binding site in SVLAC was also identified. The ability to oxidize/rearrange ethanosolv lignin further provides evidence for the utility of laccase activity for lignin degradation/modification.

Lignocellulosic biomass, composed of lignin, cellulose and hemicellulose, has been targeted as a potential source of renewable bioenergy. Lignin accounts for 20% of lignocellulosic material and is an integral part of all higher plants and the second most abundant organic polymer in nature after cellulose. Lignin serves as a key structural component and an outer protective shield against biochemical hydrolysis of the energy rich and more easily metabolizable cellulose and hemicellulose (*1, 2*). Therefore, lignin removal is required for efficient utilization of lignocellulosic biomass for the production of biofuels and other cellulose-based chemicals. Lignin has a complex, heterogeneous, polymeric structure derived from oxidative-coupling of three phenylpropanoid monomers, *p*-coumaryl, coniferyl and sinapyl alcohols (Figure S1) (*3*). The complexity of lignin structure plus its covalent connectivity to hemicellulose provides not only mechanical and structural stability but also resistance to chemical and biological degradation. Most of the available chemical pretreatment methods for lignin degradation have adverse effects on the later stages of energy conversion from cellulosic biomass and generate toxic waste products (*4-6*). For more ecologically favorable applications, methods using lignin-degrading microbes and/or their enzymes may provide a more efficient and environmentally sound approach for accessing renewable lignocellulosic biomass.

A variety of microorganisms, including certain fungi and bacteria, can degrade lignin, thus enabling access to plant carbohydrates as a rich energy source (*7-10*). Among these microorganisms white-rot fungi have attracted widespread attention because of their powerful lignin-degrading enzymatic systems (*11, 12*). However, utilization of these enzymes is problematic because of their poor stability in industrial processes, as well as the difficulty in developing efficient heterologous systems for enzyme expression and purification. Consequently, much attention has been paid to lignin degradation by bacterial species (*13-15*).

The most extensively studied are actinomycetes, particularly *Streptomyces* species because of their reported efficiency in lignin degradation, established genetic and molecular engineering tools and the availability of complete genome sequences (*16, 17*). In spite of this, very little is known about either the involvement of specific enzymes or the molecular mechanism of lignin degradation. Extensive work has been performed with *Streptomyces viridosporus* T7A in which an extracellular lignin peroxidase (LiP) was reported to possess significant lignin degradation activity (*18-20*). Despite some reports in the literature, bona fide extracellular lignin degrading peroxidases have yet to be identified in *Streptomyces viridosporus* T7A (*9, 18, 19, 21, 22*). Recently an extracellular DyP peroxidase from *Amycolatopsis sp.* 75iv2 was characterized and reported as lignin degrading enzyme (*14, 23*). Efforts to find enzymes responsible for lignin degradation by *Streptomyces* had resulted in our discovery of small laccase, a copper dependent phenol oxidase (*24*).

Laccases (p-diphenol: dioxygen oxidoreductase) are copper-containing enzymes that can oxidize a range of aromatic and non-aromatic compounds containing hydroxyl and amine groups in presence of atmospheric oxygen (*25, 26*). These enzymes are produced not only by eukaryotes such as fungi and plants but also by prokaryotes, including a wide range of Gram-positive and Gram-negative bacteria (*25, 27, 28*). Although laccases are believed to be involved in lignin synthesis in plants and in cell pigment formation, as well as metal oxidation in fungi and bacteria, their physiological roles are unclear. The most detailed biochemical characterization of laccases was done with the enzymes from the basidomycetes, *Pycnoporus cinnabarinus* and *Trametes versicolor*, wherein laccases were shown to play important roles in lignin degradation (*29, 30*). Recently, laccases from actinomycetes were reported to have *in vitro* activity against a wide range of substrates. These enzymes were designated as "small laccases" because of their

sequence similarity but smaller size compared to fungal laccases (*24*). Small laccases have been extensively exploited in the pulp and paper industries for dye-decolorization and bio-bleaching due to their high oxidizing power, pH-versatility and thermal stability (*24, 31*). Despite the advantages bacterial enzymes may offer over fungal enzymes, no detailed biochemical studies have been done using either native lignocellulosic biomass or lignin model compounds as substrates. Improved knowledge about bacterial laccases and their role in lignin degradation will have significant impact on a wide array of biotechnologies focused on lignin degradation.

The purpose of the present work is to investigate the importance of the small laccases from *Streptomyces* in both *in vivo* and *in vitro* lignin degradation activity assays using lignocellulosic biomass from *Miscanthus x giganteus,* ethanosolv lignin and *β-O-4* lignin model compounds *(3, 32)*. A *Streptomyces coelicolor* A3(2) laccase deficient mutant (SCΔLAC) was constructed to assess its *in vivo* lignin degradation activity. Using ethanosolv lignin and *β-O-4* lignin model compounds we characterized four different small laccases from *Streptomyces coelicolor* A3(2) (SCLAC), *Streptomyces lividans* TK24 (SLLAC), *Streptomyces viridosporus* T7A (SVLAC) and *Amycolatopsis sp.* 75iv2 (AMLAC) (previously known as *Streptomyces setonii* and *Streptomyces griseus* 75iv2) for their *in vitro* lignin degradation/oxidation activity. For better solubility, ethanosolv lignocellulose was used as the substrate for HPLC assays (*3*). Two different *β-O-4* lignin model compounds, with and without a phenolic group (Figure S2), were also used as substrates for spectrophotometric assays. X-ray crystal structures of small laccases, with and without substrate bound, from *Streptomyces viridosporus* T7A and *Amycolatopsis sp.* 75iv2 are also reported.

MATERIALS AND METHODS

All reagents and chemicals used as buffers and substrates were purchased of the highest grade commercially available from Sigma-Aldrich, Alfa Aesar, Acros, MP Biomedicals, or Fisher. The lignin model compounds, 1-(3, 4-dimethoxyphenyl)-2-(2-methoxyphenoxy)-1, 3-dihydroxypropane [LM-OMe, Figure S2] and 1-(3-methoxy-4-hydroxy)-2-(2-methoxyphenoxy)-1, 3-dihydroxypropane [LM-OH, Figure S2] were purchased from AstaTech, PA, USA and used as received. The ethanosolv lignin was prepared as described previously (*32*). The *Trametes versicolor* fungal laccase was purchased from Sigma-Aldrich. Enzymes for gene cloning were purchased from New England Biolabs. The buffers were made by mixing 0.1 M acetic acid, 0.1 M sodium acetate, 0.1 M potassium phosphate monobasic, 0.1 M potassium phosphate dibasic, 0.1 M sodium carbonate and 0.1 M sodium bicarbonate to the desired pH. UV-Vis spectrophotometric data were collected using a Cary 300 Bio Spectrophotometer. HPLC data were collected using Beckman Coulter System Gold Spectrophotometer. Mass Spectrometry data were collected using Shimadzu LCMS-IT-TOF. Protein purifications were done using AKTAxpress (GE) protein purification system. X-ray diffraction data were collected at Argonne National Laboratory, IL, USA.

Microorganisms. The strains of *Streptomyces coelicolor* A3(2) and *Streptomyces lividans* TK24 were kindly supplied by Prof. William W. Metcalf (University of Illinois at Urbana-Champaign) and the strains of *Streptomyces viridosporus* T7A (ATCC 39115) and *Amycolatopsis sp.* 75iv2 (ATCC 39116) were obtained from American Type Culture Collection (Rockville, MD). All strains were grown in Difco ISP Medium 1 and genomic DNAs were isolated using Wizard Genomic DNA Purification Kit (Promega) following manufacture's protocol.

Double cross-over in-frame deletion of SCO6712 by PCR targeting. The deletion of the gene encoding the *Streptomyces coelicolor* A3(2) small laccase (SCO6712) was performed following the procedures described in the REDIRECT manual (*33*). The gene was replaced with an apramycin resistance cassette, *apr*, using the PCR-targeted double cross-over in-frame deletion technique (*34*). The extended resistance cassette including *apr* resistance marker, *aac(3)IV*, was amplified from pIJ773 by PCR using SCO6712-KO-F and SCO6712-KO-R primers (Table S1). Cosmid St4C6 containing the SCO6712 gene was introduced into *E. coli* BW25113/pIJ790 (λ RED recombination plasmid) by electroporation and the resulting transformants were then electroporated with the extended resistance cassette to target the SCO6712 gene. The resulting mutant cosmid, St4C6ΔSCO6712::apr, was transformed into *E. coli* ET12567/pUZ8002 (nonmethylating strain) and then transferred into wild-type *Streptomyces coelicolor* A3(2) (SCWT), yielding the desired SCΔLAC mutant. The mutant was selected by virtue of its apramycin resistance and kanamycin sensitivity. The disruption of SCO6712 by the *apr* cassette was confirmed by PCR on the isolated genomic DNAs of both the SCΔLAC and SCWT using the primers KO-CK-F and KO-CK-R (Table S1). The mutation also was confirmed by DNA sequencing of PCR products.

Lignocellulose preparation. Miscanthus x giganteus from an experimental field at University of Illinois at Urbana-Champaign was used as the source of lignocellulose. The ground lignocellulose was prepared by passage of air-dried lignocellulose through an 80 micron sieve (SR 300 rotor beater mill, Retsch, Germany). Dry lignocellulose (3.5 g) was placed in a 1 L Erlenmeyer flask with several glass beads and autoclaved for 1 hr uncovered and then additional 30 min covered with aluminum foil.

Inoculum preparation. Spores of the SCWT or the SCΔLAC (100 μL stock) were added to 200 mL of autoclaved Difco ISP Medium 1 and incubated aerobically at 30 °C for 3 days by shaking at 220 rpm with glass beads, at which time the cells had entered into late logarithmic growth phase (*35*). The cells were collected by centrifugation, washed and resuspended in 30 mL of yeast extract-mineral salt (YEMS) medium (*35*).

Acid-precipitable polymeric lignin (APPL) production from lignocellulose. Autoclaved YEMS medium (1 L) was added to the sterile lignocellulose described previously and 10 mL of diluted log-phase cell suspension of *Streptomyces* was added; the mixture was incubated in a 2 L flask at 30 °C for one week with shaking at 220 rpm. Control reactions with YEMS medium only, YEMS medium with autoclaved lignocellulose, YEMS medium with the SCWT lacking lignocellulose and YEMS medium with the SCΔLAC strain lacking lignocellulose were performed under similar conditions. All reactions were performed in triplicate. After seven days, the residual lignocellulose and bacterial cells were removed by centrifugation. The supernatants then were acidified at 4 °C to pH 5.0 with concentrated HCl. The precipitated APPL was collected by centrifugation, air-dried, weighed and analyzed chemically.

Chemical characterization of APPL. The APPL (from the SCWT or SCΔLAC) was incubated at room temperature with 0.5 mL of 72% (w/w) sulfuric acid in a modified Hungate vial capped with a rubber stopper; the mixture was vortexed every 15 min. After 1 hr of incubation 14 mL of deionized water was added and the mixture was autoclaved for 60 min. A sugar recovery standard containing the same sulfuric acid concentration was prepared in a similar way and co-autoclaved with the samples. The mixture was kept in the refrigerator overnight and 2 mL of the clear supernatant was filtered (0.45 μm, PES) and used for high-performance liquid chromatography (HPLC) analysis.

The precipitated solids were resuspended by vortexing and the suspension was filtered through a glass micro filter. Both the vial and filter were extensively rinsed with deionized water and dried at 105 °C overnight; the weight was determined after cooling in a desiccator for 30 min. The filter and solids were then incubated at 575 °C (ramp: 105 °C for 10 min, 200 °C for 10 min, 300 °C for 30 min, 575 °C for 3 h, cooling to 105 °C); the weight was determined after cooling in desiccator for 30 min.

Calculation [Klason lignin %] = [m(filter + dried solid) – m(filter +ash)]/m(dried initial APPL) * 100 %

For ash determination, the APPL (SCWT or SCΔLAC) was incubated on a pre-weighed and conditioned aluminum pan at 575 °C (ramp: 105 °C for 10 min, 200 °C for 10 min, 300 °C for 30 min, 575 °C for 3 h, cooling to 105 °C); the weight was determined after cooling in desiccator for 30 min.

Calculation [ash %] = [m(pan + ash) – m(pan)]/m(dried initial APPL) * 100 %

For HPLC, samples were analyzed at 50 °C on an HPX-87H (300 x 7.8 mm, Bio Rad) column on an Agilent 1200 series liquid chromatography instrument equipped with a refractive index detector. Elution was performed with 0.005 M sulfuric acid at a flow rate of 0.6 mL/min.

Cloning, expression and purification of small laccases from Streptomyces coelicolor (SCLAC), Streptomyces lividans (SLLAC), Streptomyces viridosporus (SVLAC) and Amycolatopsis (AMLAC). The genes encoding the small laccase from *Streptomyces coelicolor* A3(2) (GI:21225006), *Streptomyces lividans* TK24 (GI:256783840), *Streptomyces viridosporus* T7A (GI:2518361192) and *Amycolatopsis sp.* 75iv2 (GI:2513525025) were PCR-amplified from their corresponding genomic DNA without TAT secretion tag, with the primers (Integrated DNA

technologies) listed in Table S1 and all of which had a 5′-*Nde*I restriction site and 3′-*Bam*HI restriction site, respectively. The PCR mixture (50 µL) contained 5 µL of 5 ng/µL template genomic DNA, 10 µL of Expand High Fidelity^{PLUS} reaction buffer (5X) with 7.5 mM $MgCl_2$, 2 µL 10 mM dNTP mixture, 2.5 µL DMSO, 2 µL of each 20 µM forward and reverse primers, 1 µL Expand High Fidelity^{PLUS} (5 U/µL) enzyme blend (Roche) and 25.5 µL of ddH_2O. The PCR were performed in a Veriti 96 Well Thermal Cycler (Applied Biosystems) with the following parameters: 94 $^{\circ}$C for 4 min followed by 35 cycles of 94 $^{\circ}$C for 30 sec, 70 $^{\circ}$C for 45 sec, 72 $^{\circ}$C for 1.15 min and the final extension time was 7 min at 72 $^{\circ}$C. The PCR products were purified by gel extraction (Qiagen) following the manufacturer's protocol. The amplified DNA products were digested with *Nde*I and *Bam*HI restriction enzymes (New England Biolabs) and ligated into pET15b expression vector (Novagen) cut with the same enzymes. The N-terminal His tagged proteins were expressed in *E. coli* BL21 (DE3) cells at 30 $^{\circ}$C. A bacterial culture for a typical preparation utilized 4 x 1 L of LB medium shaken at 37 $^{\circ}$C until the OD_{600} reached 0.6 after which it was induced with 1 mM IPTG. The culture was then shaken at 30 $^{\circ}$C for another 20 h and harvested by centrifugation. The cell pellets were resuspended in 50 mL of buffer containing 5 mM imidazole, 500 mM NaCl and 20 mM Tris-HCl (pH 7.9). The suspension was sonicated to lyse the cells and the lysate was cleared by centrifugation. The supernatant was applied to a 5 mL HisTrap^{TM} HP column (GE Healthcare) and eluted with a linear gradient (100 mL) of 0 to 1 M imidazole buffered with 500 mM NaCl and 20 mM Tris-HCl (pH 7.9). Fractions containing the small laccase was collected and dialyzed against 1X PBS (Phosphate Buffered Saline) buffer (pH 7.4) containing 137 mM NaCl, 2.7 mM KCl, 10 mM Na_2HPO_4 and 1.76 mM KH_2PO_4. After cleavage of the N-terminal His-tag by thrombin (GE Healthcare) at room temperature, the proteins were dialyzed against 20 mM Tris-HCl (pH 7.9) before being applied to a 5 mL

HiTrap™ Q HP column (GE Healthcare). The proteins were eluted with a linear gradient (100 mL) of 0 to 1 M NaCl buffered with 20 mM Tris-HCl (pH 7.9). Fractions containing pure (> 95%) proteins were collected and dialyzed twice against 20 mM Tris-HCl (pH 7.9) containing $CuSO_4$ at four fold greater molar ratio to given 4 copper atoms per active site and then stored at -80 °C.

Determination of laccase activity at different pH. The small laccase activities at different pH (3-10) were determined at 25 °C using 2,2′-azino-bis(3-ethylbenzothiazoline-6-sulfonate) [ABTS] or 2,6-dimethoxy phenol [DMP] as the substrate. The oxidation of substrates was detected by measuring the absorbance at 420 nm for ABTS (ε_{420} = 36000 M^{-1} cm^{-1}) at pH 3-5 and at 468 nm (ε_{468} = 14800 M^{-1} cm^{-1}) for DMP at pH 6-10. The reaction mixture (200 μL) contained 10 mM ABTS (dissolved in water) and 5 mM DMP (dissolved in DMF) and the small laccase (2.0 μM) with the appropriate buffer, respectively.

Determination of k_{rel} and K_{app} of small laccases. LM-OH, a phenolic *β-O-4* lignin-model compound (Figure S2), was used as lignin-model substrate to determine k_{rel} and K_{app} of small laccases. Spectrophotometric assays were performed at room temperature and monitored at 340 nm (ε_{340} = 1500 M^{-1} cm^{-1} for the formation of vanillin, one of the LM-OH oxidation products, Figure S9). Reaction mixtures (200 μL) were buffered at varying pH (6-10) with 100 mM potassium phosphate buffer (pH 6-8) and 100 mM sodium carbonate buffer (pH 9-10). It contained 1-100 mM LM-OH (dissolved in DMF) as substrate and the enzyme (20-30 μM) at room temperature. The steady-state kinetic parameters were evaluated by fitting the initial rates in Michaelis-Menten equation using GraphPad Prism (*36*).

Ethanosolv lignin degradation by small laccase. In order to detect activity of small laccase with a heterogeneous mixture of lignin building blocks, the enzyme was incubated for 16 h in the presence of ethanosolv lignin. The resultant cloudy reaction mixture with some precipitate was mixed vigorously while adding an equal volume of 20% acetonitrile (CH_3CN) in water to a final concentration of 10% to produce a homogeneous suspension. The mixture containing 10% CH_3CN was then centrifuged for 10 min at 15,000g. Cleared supernatant was applied to a C18 column (μBondapak™ C18, 10 μM 125 Å, 4.6 x 150 mm, Waters) and eluted with a 10% isocratic gradient of CH_3CN/H_2O for 5 mL, followed by a linear gradient of 10-60% for 25 mL at a flow rate of 1 ml/min and monitored at 285 nm.

Size exclusion chromatography was utilized to elucidate the relative size distribution of small laccase degraded ethanosolv lignin. For size exclusion, the cloudy reaction mixture was mixed with an equal volume of 60% CH_3CN/H_2O to solubilize the otherwise insoluble lignin species. A sample (20 μL) was then injected into size exclusion column (BioSuite™ 125, 4 μM UHR SEC, 4.6 x 300 mm, Waters) with a mobile phase consisting of 30% CH_3CN/H_2O, eluted at 0.4 mL/min and monitored at 315 nm.

Crystallization and data collection for AMLAC. Two crystal forms of *Amycolatopsis sp.* 75iv2 small laccase (AMLAC) were obtained utilizing the Hampton Research sparse matrix crystallization screens. Crystals were obtained both in the presence and absence of a non-phenolic *β-O-4* lignin model compound (LM-OMe) [Figure S2]. Both crystal forms appeared within two weeks of the initial setup in the Crystal Screen II condition #3 and Index Screen condition #11. Centered orthorhombic crystals were obtained in the presence of the LM-OMe substrate analogue in the first and rhombohedral ligand-free crystals in the second condition, respectively, using the hanging drop vapor diffusion method at 4 ˚C.

For the crystals of AMLAC•Cu^{2+}•LM-OMe (PDB 3TA4), the protein solution contained AMLAC (20 mg/mL) in 20 mM Tris-HCl (pH 7.9) and 20 mM of LM-OMe ligand; the precipitant contained 25% ethylene glycol. Crystals appeared within two weeks and exhibited diffraction consistent with the space group $C222_1$, with three molecules per asymmetric unit. Prior to data collection, the crystals were dipped in fresh mother liquor, followed by flash cooling in liquid nitrogen; the ligand was not included in cryoprotectant solution.

For the crystals of AMLAC•Cu^{2+} (PDB 3T9W), the protein solution contained AMLAC (20 mg/mL) in 20 mM Tris-HCl (pH 7.9); the precipitant contained 3.0 M NaCl and 100 mM Hepes (pH 7.5). Crystals appeared within two weeks and exhibited diffraction consistent with the space group R32, with one molecule per asymmetric unit. Prior to data collection, the crystals were immersed in a cryoprotectant solution composed of 30% glycerol and of 70% of the original mother liquor. After 30 seconds of incubation, the crystals were vitrified by immersion in liquid nitrogen.

The diffraction data for AMLAC•Cu^{2+} was recorded at LS-CAT (Sector 21 ID-G, Advanced Photon Source, Argonne, IL) using a MAR 300 CCD detector. The diffraction data for AMLAC•Cu^{2+}•LM-OMe was recorded at LS-CAT (Sector 21 ID-F, Advanced Photon Source, Argonne, IL) using a MAR 225 CCD detector. Diffraction intensities were integrated and scaled with the XDS package (*37*). Relevant data collection and data reduction statistics are given in Table 4.

Crystallization and data collection for SVLAC. Two crystal forms were also obtained for the *Streptomyces viridosporus* T7A small laccase (SVLAC). Approximately one month after the initial setup of the Precipitant Synergy sparse matrix screen, orthorhombic crystals appeared in condition #16, and trigonal crystals in condition #8, using the hanging drop vapor diffusion

method at 9 ˚C. The trigonal crystal form was also subjected to soaking experiments with acetovanillone (AV), a naturally occurring mediator (*38, 39*). Although cocrystallization with the LM-OMe compound was attempted, no ligand was detected in resultant electron density maps for either of the two crystal forms. The presence of the Zn^{2+} atom in the first crystal form was established via the identities of its binding-residues (*40*). In addition, zinc content of the enzyme was analyzed with Sciex Elan DRCe ICP-MS (Perkin Elmer) at the University of Illinois Microanalytical Laboratory.

For the crystals of SVLAC•Cu^{2+}•Zn^{2+} (PDB 3TBB), the protein solution contained SVLAC (20 mg/mL) in 50 mM Hepes-K^+ (pH 8.0) and 100 mM KCl; the precipitant contained 2.0 M Li_2SO_4, 5% polyethylene glycol 400, 100 mM $MgSO_4$ and 100 mM acetate (pH 5.5). Crystals appeared in approximately one month and exhibited diffraction consistent with the space group I222, with three molecules per asymmetric unit. Prior to data collection, the crystals were immersed in a cryoprotectant solution composed of 4.0 M Na-malonate. After 30 seconds of incubation, the crystals were vitrified by immersion in liquid nitrogen.

For the crystals of SVLAC•Cu^{2+} (PDB 3TAS) and SVLAC•Cu^{2+}•AV (PDB 3TBC), the protein solution contained SVLAC (20 mg/mL) in 20 mM Tris-HCl (pH 7.9); the precipitant contained 5% 2-propanol and 2.5 M dibasic potassium phosphate/monobasic sodium phosphate (pH 5.5). Crystals appeared in approximately one month and exhibited diffraction consistent with the space group $P3_121$, with three molecules per asymmetric unit. Prior to data collection, the crystals of SVLAC•Cu^{2+} were immersed in a cryoprotectant solution composed of 70% of the original mother liquor and 30% of glycerol. After 30 seconds of incubation, the crystals were vitrified by immersion in liquid nitrogen. For SVLAC•Cu^{2+}•AV, the ligand-free crystals were transferred into fresh mother liquor containing 20 mM acetovanillone and incubated at 9˚ C for

four hours. The crystals were vitrified as described earlier and the cryoprotectant solution did not contain the ligand.

The diffraction data set for SVLAC•Cu^{2+}•Zn^{2+} was recorded at LS-CAT (Sector 21 ID-G, Advanced Photon Source, Argonne, IL) using a MAR 300 CCD detector. The diffraction data set for the crystals of SVLAC•Cu^{2+} and SVLAC•Cu^{2+}•AV were recorded at LS-CAT (Sector 21 ID-F, Advanced Photon Source, Argonne, IL) using a MAR 225 CCD detector. Diffraction intensities were integrated and scaled with the XDS package (*37*). The data collection statistics are given in Table 4.

Structure determination and model refinement for AMLAC and SVLAC. The structures of both liganded and unliganded AMLAC and SVLAC were solved by molecular replacement with PHASER (*41*), using the atomic coordinates of the small laccase from *Streptomyces coelicolor* A3(2) (PDB 3CG8) as the search model. The partial solution from PHASER was then subjected to automated model building with ARP/wARP (*42*), followed by multiple iterative cycles of manual and automated rebuilding with COOT (*43*), interspersed with rounds of refinement using PHENIX (*44*). Water molecules were automatically built with ARP/wARP, followed by manual assessment in COOT. Final refinement statistics are provided in Table 4 and Table 5.

RESULTS AND DISCUSSION

Identification of the small laccase. The genome of *Streptomyces coelicolor* A3(2) encodes a "small" laccase (SCLAC) that is homologous to fungal laccases, although the bacterial laccase contains two domains and the larger fungal laccases contain three domains. The gene encoding SCLAC is genome proximal (separated by eight genes) to a seven-gene operon encoding enzymes in the β-ketoadipate pathway to the tricarboxylic acid cycle intermediates acetyl-CoA and succinyl-CoA (*45*). Homologous gene clusters can be found in the genomes of

several *Streptomyces* species, including *Streptomyces lividans* TK24, *Amycolatopsis sp.* 75iv2 and *Streptomyces griseus* NBRC 13350. Because lignin is composed of aromatic moieties, we investigated whether SCLAC is involved in lignin degradation (*24, 31*) by disruption of the gene encoding the small laccase by insertion of an apramycin resistance cassette, *apr*, using PCR-targeted *Streptomyces* gene replacement method, yielding the mutant designated SCΔLAC.

Lignocellulose degradation by the small laccase. Quantitative studies of lignin degradation are hampered by the lack of convenient assay methods due to the complexity and heterogeneity of its polymeric structure (Figure S1). The mineralization of lignin can be quantified by the conversion of ^{14}C-labeled lignin to $^{14}CO_2$. However, this method requires the biosynthetic preparation of the isotopically labeled substrate and, therefore, may allow for the incorporation of radioactivity into non-lignin components of the lignocellulose, e.g. proteins, aromatic acids esterified to hemicelluloses or to lignin and other aromatics such as lignans (*8*). Also, a spectrophotometric assay recently was reported using chemically nitrated lignin, but the assay sensitivity is low and we were unable to demonstrate lignin degradation using this method (*46*). Monomeric and *β-O-4* dimeric lignin model compounds have been used, but these are not perfect representations of the complex native lignin structures (*47*). Finally, some organisms show lignin degradation activity only in the presence of cellulosic biomass, i.e. in native lignocellulosic state (*48*). Therefore, we considered the use of native lignocellulose, a combination of lignin, cellulose and hemicellulose, as an important real-world criterion for determining the lignin degradation activity of microorganisms.

Considering the molecular size and structure of lignin, it is reasonable to postulate that its microbial degradation will involve extracellular (secreted) enzymes. Actinomycetes are known to secrete enzymes that produce water soluble, polymeric lignin fragments from different

lignocellulosic materials. These intermediates precipitate from aqueous solution upon acidification and are known as acid-precipitable polymeric lignin (APPL) (*35*). Quantification of APPL production can provide a measure of the lignin degradation efficiency; chemical characterization of the APPL has the potential to elucidate the molecular processes involved in lignin degradation (*35*). We reasoned that if the small laccase is involved in lignin degradation, less APPL would be produced by the SCΔLAC mutant than by the wild type strain SCWT. Also, chemical analysis of the APPL produced by the mutant and wild type strains would provide a measure of the extent of lignin degradation and therefore the importance of the small laccase in the APPL production.

APPL production assays were performed with the SCWT and SCΔLAC mutant strains using milled, air-dried lignocellulose from *Miscanthus x giganteus* as the source of lignin substrate (*3*). Controls were performed using **i)** the medium alone, **ii)** the medium with lignocellulose and **iii)** the medium with either the SCWT or SCΔLAC mutant strain in the absence of lignocellulose. The growth of SCWT and SCΔLAC mutant strains were similar under experimental conditions (the growth was measured by monitoring the OD at 600 nm). After one week of incubation the residual lignocellulose and bacteria were removed by centrifugation. The supernatants were acidified at 4 $^{\circ}$C to minimize acid hydrolysis and the resulting precipitates (APPL) were dried and weighed. APPL was found only in the supernatants of the cultures containing both bacteria and lignocellulose but not in any of the control experiments (Figure 1). This indicates that APPL is the breakdown product of lignocellulosic substrates in the presence of the SCWT and SCΔLAC mutant strains and not a hydrolysis product of lignocellulose.

Although the SCΔLAC strain produced APPL, the total amount of APPL was significantly less (33.1%) than that produced by the wild type strain (Table 1). That the mutant was deficient in APPL production may support the possible importance of the small laccase in lignin degradation. The results of the compositional characterization and chemical analysis of the APPLs produced by the SCWT and SCΔLAC strains are shown in Table 2. The results are the mean of triplicate analysis, except for ash (duplicate analysis) and nitrogen (single analysis). The level of lignin degradation (Klason lignin) as measured from the total amount of APPL produced by SCWT was much greater than that produced by the SCΔLAC strain (Table 2). As a result of the larger extent of lignin degradation by the SCWT strain a larger amount of carbohydrate (glucan, xylan and arabinan) was released by the SCWT strain (15.9 mg) than by the SCΔLAC strain (11.9 mg), suggesting the hydrolytic enzymes had easier access to the carbohydrate biomass. The acetyl content of the APPL quantitates the acetyl released from acetyl esters of both lignin and hemicellulose; the larger amount of acetyl released by the SCWT strain again suggests higher accessibility to the carbohydrate biomass due to the greater lignin degradation by the SCWT strain. Ash and nitrogen measure the amounts of inorganic salts and protein present in APPL, respectively, and were unchanged by the disruption of the gene encoding the small laccase (Table 2).

Functional characterization of purified small laccases. To investigate further the involvement of small laccases in lignin degradation, four small laccase enzymes, SCLAC, SLLAC, SVLAC and AMLAC, were expressed and purified from *E. coli* with a high yield (15-20 mg/L cell culture). SDS-PAGE of pure laccase enzymes show both monomeric and trimeric form, an observation found previously (Figure S8) (*24*). They are very stable enzymes that are active across a broad pH range (pH 3-10), compared to fungal laccases which are mostly active

at low pH (*49, 50*). Their activities were determined using ABTS (pH 3-5) and DMP (pH 6-10) as substrates (data not shown). The high yields of the small laccases from *Streptomyces* using *E.coli* as heterologous expression system and their stability over a broad pH range make them excellent candidates for various industrial applications.

Oxidative degradation of lignin model compounds. Both phenolic and non-phenolic dimeric *β-O-4* lignin model compounds are widely used to study C_α-C_β bond cleavage in lignin degradation (*8*). The ability of small laccases to degrade/oxidize the dimeric *β-O-4* lignin model compounds indirectly reflects their ability of lignin oxidative degradation, as more than 50% of lignin structure is comprised of *β-O-4* bonds (*3*). Scheme S1 demonstrates a possible oxidative degradation pathway of *β-O-4* lignin model compounds by laccases. It was postulated that laccase is only responsible for the radical initiation step, with the downstream C-C bond deconstruction the result of spontaneous reactions (*51*). The catalytic activities of the *Streptomyces* laccases were determined by measuring the release of degradation product(s) due to the C_α-C_β bond cleavage/rearrangement of the LM-OH phenolic *β-O-4* lignin model compound at pH 8.0 and at 25 $^\circ$C. A mixture of oxidative degradation products was formed, which were not fully characterized. However, one of the products was identified and characterized as vanillin which absorbs at 340 nm (Figure S9). Product(s) formation at this wavelength was found to show Michaelis-Menten kinetics, and thereby the relative k_{cat} (k_{rel}) and apparent K_M (K_{app}) values were calculated for small laccases (Table 3). The low k_{rel}/K_{app} (low k_{rel} and high K_{app}) values suggest that the *β-O-4* model compound is not the natural substrate, prompting us to use the slightly modified native lignin substrate (ethanosolv lignin) for further studies. The pH optimum for SCLAC against LM-OH was determined; the values of k_{rel} and k_{rel}/K_{app} were highest at pH 8.0 (Figure S3). Different mediators, ABTS and HOBt, were used to

oxidize non-phenolic *β-O-4* lignin model compound (LM-OMe) in presence of small laccases. No C_α-C_β bond cleavage were observed, instead there was very slow formation of the corresponding ketone product [Figure 2, identified by MS (Figure S7)], a behavior previously observed with fungal laccase (*52*). However, the rate of conversion of LM-OMe to quinone product by small laccases was slower compared to fungal laccase from *T. versicolor* (data not shown). This result suggests that even in the presence of mediators neither bacterial nor fungal laccases were able to cleave the C_α-C_β bond of LM-OMe compound, but they were able to modify the structure by forming the quinone product at different rates. These activities explains laccases' role in enhancing the access of energy rich cellulose and hemicellulose by modifying lignin structure (*16*).

Degradation/modification of ethanosolv lignin. To verify the activity of the laccases against native lignin, ethanosolv lignin was used because of its better water solubility. Ethanosolv lignin was prepared by pre-treating native *Miscanthus* lignocellulose with 80% aqueous ethanol and 0.5% w/w (based on raw material dried mass) sulfuric acid as catalyst at high temperature (*2, 32*). Ethanosolv lignin retains the same lignin and carbohydrate composition as native lignocellulose except that the molecular weight is lower, which makes it more water soluble and convenient for enzyme assays (*2*). After reacting ethanosolv lignin with purified SCLAC for 16 h at 37 $^{\circ}$C, the reaction mixture was passed through a reverse phase C18 column; the elution profile is shown in Figure 3. As determined by LC-MS, most of the ionizable peaks from this elution profile belong to a molecular weight range of 200-1000 Da. The major species (~ 13 min) was determined, by Agilent 1100 LC/MSD Trap XCT Plus (LC/MS) at the University of Illinois Roy J. Carver Biotechnology center, to be *p*-coumaric acid ethyl ester with a molecular weight of 192.08, an expected lignin degradation product and a natural laccase

mediator (*53, 54*). The chromatogram seems to indicate loss of soluble material, which can be equated to polymerization of the smaller lignin units into larger pieces that are less soluble in aqueous solution and were not retained during work up on the reaction mixture for C18 chromatography (*vide infra*). It is believed that laccases catalyze the oxidation of lignocellulosic substrates to produce aryl cation radicals; these radicals spontaneously rearrange, leading to further polymerization of degraded materials by the fission of carbon-carbon or carbon-oxygen bonds of the alkyl side chains or to the cleavage of aromatic rings (*55, 56*). Taking this into account, our experiments aimed at reproducing natural lignin biodegradation *in vitro* indicate that although the laccase is able to degrade lignin substrates, the products simultaneously undergo competing radical polymerization.

To probe this conclusion, size-exclusion chromatography was utilized to elucidate the relative size distribution of ethanosolv lignin after reaction with SCLAC. The results are shown in Figure 4. For this experiment, unlike the reverse phase C18 column chromatography experiment, the cloudy reaction mixture was mixed with an equal volume of 60% CH_3CN/H_2O to solubilize the polymerized lignin species. An observable shift towards larger molecular weight lignin was observed, as was expected based on the loss of material in the C18 chromatograms (*vide supra*). Due to the lack of appropriate molecular weight standards, the molecular weight estimate is only qualitative. Nevertheless, we can conclude that during *in vitro* lignin degradation there is competition between de-polymerization and re-polymerization, which would shift toward de-polymerization under *in vivo* conditions due to presence of a suitable radical quencher (*56*). Considering the very complex structure of lignin and the subsequent complexity of re-condensation of reactive lignin degradation products, it is unlikely that this biopolymer can be effectively degraded by one enzyme alone. In fungi, FAD-dependent enzymes veratryl alcohol

oxidase and glucose 1-oxidase were considered to have co-operative action with laccase to prevent the re-polymerization by reducing the reactive radical species (*51, 56*). For *Streptomyces* discovery of such a co-operative enzyme for prevention of re-polymerization is an area of active study.

Structure of small laccases. A multiple sequence alignment of all four small laccases shows that all the active site residues involved in copper binding are conserved (Figure S4). These residues are also highly conserved among other laccases and four-copper oxidases from fungi, plants and bacteria although there is less similarity across the rest of the protein (*24*).

Laccases are known to bind four copper ions (II) in three different binding sites, each characterized by unique spectroscopic properties and playing an important role in substrate oxidation (*31, 57-60*). The paramagnetic Type-1 (T1) copper is coordinated by two His residues, one Met residue and one Cys residue. The tight coordination of T1 copper to Cys residue is responsible for an intense absorption band around 600 nm, giving the blue color to the enzyme. Two His residues are coordinated to one paramagnetic Type-2 (T2) copper and three His residues (six His residues total) are coordinated to each of the two Type-3 (T3) coppers. The T3 coppers are antiferromagnetically coupled with EPR silent pair absorption maximum at 330 nm. The one T2 and two T3 coppers are arranged in a trinuclear cluster, which is believed to be the site of molecular oxygen reduction (*31, 57*). The catalytic cycle is thought to be initiated by oxidation of substrate near the T1 copper site by transfer of an electron from the substrate. In total, four electrons (produced by oxidation of four substrates) are then sequentially transferred from the T1 copper to the trinuclear cluster along a Cys-His pathway, where one oxygen molecule is reduced to two water molecules to complete the cycle (*31*).

The structure of AMLAC was solved both in the presence (PDB 3TA4) and absence (PDB 3T9W) of a non-cleavable lignin *β-O-4* model compound LM-OMe (Figure S2). Although the biologically active form of the enzyme is a trimer, the ligand-free structure (space group R32) contains one molecule per asymmetric unit. In this case the crystallographic symmetry-related molecules complete the trimeric composition. To date, the unliganded structure of AMLAC reported here (PDB 3T9W) is the highest resolution structure of a small bacterial laccase. The enzyme shares 58% sequence identity to the previously reported small laccase from *Streptomyces coelicolor* A3(2) (PDB: 3CG8 and 3KW8) (SCLAC) and consists of an identical two-domain fold with metal-binding architecture (*31*).

The T1 copper-binding site contains a highly ordered copper ion that is coordinated to Cys 279, His 222, and His 284 with Met 298 as the axial ligand. The T2 copper is coordinated to His 93 and *His 225 (where the * denotes the residue from a symmetry-related polypeptide). The first T3 copper is coordinated to His 95, His 147 and *His 280; the second T3 copper site is made up of His 149 and *His 278 and *His 227. The area between the T2 and T3 copper centers contains strong positive electron density in the (F_o-F_c) omit map, suggestive of a bound dioxygen molecule. However, the electron density is elongated so a hydrogen peroxide molecule may be more appropriate. This dioxygen reduction intermediate, however, is not unusual and has previously been reported in three-domain laccase structures with almost identical coordination geometry (Figure S5) (*61, 62*).

Whereas the three-domain laccases contain a negatively charged Glu or Asp residue in the tip of the access solvent channel, the water molecule coordinated to O1 of the peroxide is bonded to a polar Gln 282 residue in the AMLAC structure. The ligand-bound structure of AMLAC (PDB 3TA4) (space group $C222_1$) contains three polypeptides in the asymmetric unit.

The trimer contains three trinuclear and three mononuclear copper centers. Serendipitously, this crystal form allows for the binding of the non-phenolic lignin model compound LM-OMe, which was included in the crystallization solution. Although the surface of the trimer lacks defined cavities that may act as the binding pocket for small-molecule phenolic substrates, it is conceivable that the rather flat trimer surface is optimal for binding large phenolic polymers. Although it is questionable whether the binding of the model compound is biologically relevant, its binding site is close to the T1 copper site, which is believed to be the main source of catalytic activity for the oxidation of phenolic compounds (*63, 64*). The ligand in this crystal form is trapped in a "wedge" between two crystallographic symmetry-related trimers (Figure 5). It is also not possible to assess the orientation of the inert substrate molecule due to its three-dimensional conformation, which is nearly symmetric (Figure 5). The ligand was modeled at an occupancy of 0.46 as the molecule lies on a symmetry axis and occupies approximately half of the site. The site lying between the T2 and T3 copper atoms that was occupied by a hydrogen peroxide moiety in the ligand-free structure contains a water molecule.

Structures of SVLAC were solved in two distinct crystal forms. SVLAC shares 87% sequence identity to SCLAC and differs mainly in the sequence of the C-terminal tail of the enzyme. Both crystal forms are composed of asymmetric units that contain the biologically active trimeric enzyme. However, regions that were ordered in the crystal form belonging to I222 space groups were disordered in the crystals belonging to $P3_121$ space group due to crystal packing. However, the hexagonal crystal form produced a condition similar to that of the trimeric form of AMLAC, enabling the trapping of a substrate molecule at the crystallographic symmetry-related trimer interface. The new feature that can be observed with the structure

belonging to the I222 space group is the extra metal-binding site (PDB 3TBB), which arises from an insertion of two extra histidine residues in the C-terminus that SCLAC lacks.

Based on the results from the ICP-MS analysis, we hypothesize that this site contains a zinc ion. The binding pocket for the zinc ion is formed by Glu 158 and His 159 of one polypeptide and a *His 315 residue of the neighboring polypeptide. In all three zinc binding sites in the trimer, the metal ion is within ~2.3Å of the ε-nitrogen of the histidine residues and within ~2.6Å of the carboxylate oxygen of the glutamate moiety. In each of the three sites, the zinc ion is also coordinated to at least one water molecule (Figure S6). .

In the structure, the mono- and tri- nuclear copper sites are conserved. The T1 copper-binding site contains a highly ordered copper ion that is coordinated to Cys 283, His 226, and His 288 with Met 293 as the axial ligand. The T2 copper is coordinated to His 97 and *His 229. The first T3 copper is coordinated to His 99, His 151 and *His 284; the second T3 copper site is made up of His 153 and *His 282 and *His 231. The site that was occupied by a hydrogen peroxide in the high-resolution structure of AMLAC contains a dioxygen molecule in all three polypeptides of SVLAC. Interestingly, a molecule of acetate, a component of the crystallization buffer, is coordinated to one of the T3 copper atoms in all three polypeptides. The trigonal crystal form, which lacks the C-terminal tail involved in zinc coordination, was an excellent candidate for soaking experiments.

Although multiple natural mediators were tested in soaking experiments, only acetovanillone (AV) yielded detectable electron density in the resultant structure. Although the presence of AV is again most likely attributable to crystal packing, this phenolic substrate is bound only ~10Å away from the T1 copper site. The binding of AV, when compared to the LM-OMe binding to AMLAC, seems to be more specific with multiple hydrogen-bonding

interactions to the SVLAC polypeptide. The molecule of AV is stacked against what appears to be a molecule of Tris from the purification buffer (Figure 6). The Tris, however, is ordered only in the liganded structure and is missing from the electron density in the apo-form of this crystal form.

Conclusions. We provided evidence that **1)** strains of *Streptomyces* that encode the small laccase have the potential to be useful in lignin degradation, and **2)** the extracellular small laccase plays an important role in this process. The small laccases from four different *Streptomyces* were cloned, expressed and purified from heterologous sources and proved to be stable and active against different substrates under versatile pH conditions. These enzymes were able to degrade phenolic *β-O-4* lignin model compound without any mediators and rearrange non-phenolic *β-O-4* lignin model compound in presence of mediators, which provide *in vivo* validation for their lignin degradation activity. However, APPL production was not completely eliminated by the laccase deficient strain, so other, to be discovered, enzymes likely are also involved in lignin degradation.

SUPPORTING INFORMATION

Primers used in this study (Table S1), Structural motif of lignin (Figure S1), Lignin model compounds (Figure S2), Dependence of steady-state kinetic parameters of SCLAC on pH (Figure S3), Multiple sequence alignment of small laccases (Figure S4), Coordination geometry of the H_2O_2 intermediate bound to the trinuclear center copper atoms and water molecules in AMLAC (Figure S5), The zinc metal-ion binding site of SVLAC (Figure S6), ESI-MS showing the formation of ketone derivative (Figure S7), SDS-PAGE of purified small laccases (Figure S8), ESI-MS showing the formation oxidative products (Figure S9), Proposed oxidative mechanism of lignin model compound (Scheme S1). "This material is available free of charge via the Internet at http://pubs.acs.org."

ACCESSION CODES

PDB entries: 3TA4 (AMLAC•Cu^{2+}•LM-OMe), 3T9W (AMLAC•Cu^{2+}), 3TBB (SVLAC•Cu^{2+}•Zn^{2+}), 3TAS (SVLAC•Cu^{2+}), 3TBC (SVLAC•Cu^{2+}•AV)

REFERENCES

1. Adler, E. (1977) Lignin chemistry - past, present and future, *Wood Sci. Technol. 11*, 169-218.
2. El Hage, R., Chrusciel, L., Desharnais, L., and Brosse, N. (2010) Effect of autohydrolysis of Miscanthus x giganteus on lignin structure and organosolv delignification, *Bioresour Technol 101*, 9321-9329.
3. Villaverde, J. J., Li, J., Ek, M., Ligero, P., and de Vega, A. (2009) Native lignin structure of *Miscanthus x giganteus* and its changes during acetic and formic acid fractionation, *J. Agric. Food Chem. 57*, 6262-6270.
4. Klinke, H. B., Thomsen, A. B., and Ahring, B. K. (2004) Inhibition of ethanol-producing yeast and bacteria by degradation products produced during pre-treatment of biomass, *Appl. Microbiol. Biotechnol. 66*, 10-26.
5. Palmqvist, E., and Hahn-Hagerdal, B. (2000) Fermentation of lignocellulosic hydrolysates. I: inhibition and detoxification, *Bioresour. Technol. 74*, 17-24.
6. Palmqvist, E., and Hahn-Hagerdal, B. (2000) Fermentation of lignocellulosic hydrolysates. II: inhibitors and mechanisms of inhibition, *Bioresour. Technol. 74*, 25-33.
7. Ander, P., and Eriksson, K. E. (1978) Lignin degradation and utilization by microorganisms, *Prog. Ind. Microbiol. 14*, 1-58.
8. Kirk, T. K., and Farrell, R. L. (1987) Enzymatic "combustion": the microbial degradation of lignin, *Annu Rev Microbiol 41*, 465-505.
9. Moyson, E., and Verachtert, H. (1993) Microbial degradation of lignin, *Meded. - Fac. Landbouwkd. Toegepaste Biol. Wet. (Univ. Gent) 58*, 1651-1653.

10. Abdel-Hamid, A. M., Solbiati, J. O., and Cann, I. K. (2013) Insights into lignin degradation and its potential industrial applications, *Adv. Appl. Microbiol. 82*, 1-28.

11. Kirk, T. K. (1981) Principles of lignin degradation by white-rot fungi, *Ekman-Days 1981, Int. Symp. Wood Pulping Chem. 3*, 66-70.

12. Tuor, U., Winterhalter, K., and Fiechter, A. (1995) Enzymes of white-rot fungi involved in lignin degradation and ecological determinants for wood decay, *J. Biotechnol. 41*, 1-17.

13. Iyer, A. P., and Mahadevan, A. (2002) Lignin degradation by bacteria, *Prog. Ind. Microbiol. 36*, 311-330.

14. Brown, M. E., Walker, M. C., Nakashige, T. G., Iavarone, A. T., and Chang, M. C. (2011) Discovery and characterization of heme enzymes from unsequenced bacteria: application to microbial lignin degradation, *J. Am. Chem. Soc. 133*, 18006-18009.

15. Bugg, T. D., Ahmad, M., Hardiman, E. M., and Singh, R. (2011) The emerging role for bacteria in lignin degradation and bio-product formation, *Curr. Opin. Biotechnol. 22*, 394-400.

16. Kirby, R. (2006) Actinomycetes and lignin degradation, *Adv. Appl. Microbiol. 58*, 125-168.

17. Crawford, D. L. (1986) The role of actinomycetes in the decomposition of lignocellulose, *Symp. Biol. Hungar. 32*, 715-728.

18. Ramachandra, M., Crawford, D. L., and Hertel, G. (1988) Characterization of an extracellular lignin peroxidase of the lignocellulolytic actinomycete *Streptomyces viridosporus*, *Appl. Environ. Microbiol. 54*, 3057-3063.

19. Thomas, L., and Crawford, D. L. (1998) Cloning of clustered *Streptomyces viridosporus T7A* lignocellulose catabolism genes encoding peroxidase and endoglucanase and their extracellular expression in *Pichia pastoris*, *Can. J. Microbiol. 44*, 364-372.

20. Wang, Z., Bleakley, B. H., Crawford, D. L., Hertel, G., and Rafii, F. (1990) Cloning and expression of a lignin peroxidase gene from *Streptomyces viridosporus* in *Streptomyces lividans*, *J. Biotechnol. 13*, 131-144.

21. Godden, B., Ball, A. S., Helvenstein, P., McCarthy, A. J., and Penninckx, M. J. (1992) Towards elucidation of the lignin degradation pathway in actinomycetes, *J. Gen. Microbiol. 138*, 2441-2448.

22. Ramachandra, M., Crawford, D. L., and Pometto, A. L. (1987) Extracellular Enzyme Activities during Lignocellulose Degradation by *Streptomyces spp.*: A Comparative Study of Wild-Type and Genetically Manipulated Strains, *Appl. Environ. Microbiol. 53*, 2754-2760.

23. Brown, M. E., Barros, T., and Chang, M. C. (2012) Identification and characterization of a multifunctional dye peroxidase from a lignin-reactive bacterium, *ACS Chem. Biol. 7*, 2074-2081.

24. Machczynski, M. C., Vijgenboom, E., Samyn, B., and Canters, G. W. (2004) Characterization of SLAC: A small laccase from *Streptomyces coelicolor* with unprecedented activity, *Protein Sci. 13*, 2388-2397.

25. Gianfreda, L., Xu, F., and Bollag, J.-M. (1999) Laccases: A useful group of oxidoreductive enzymes, *Biorem. J. 3*, 1-25.

26. Mayer, A. M., and Staples, R. C. (2002) Laccase: new functions for an old enzyme, *Phytochemistry 60*, 551-565.

27. Dwivedi, U. N., Singh, P., Pandey, V. P., and Kumar, A. (2011) Structure-function relationship among bacterial, fungal and plant laccases, *J. Mol. Cat. B: Enz. 68*, 117-128.

28. Ferrer, M., Beloqui, A., and Golyshin, P. N. (2010) Screening metagenomic libraries for laccase activities, *Methods Mol. Biol. (New York, NY, United States) 668*, 189-202.

29. Youn, H.-D., Hah, Y. C., and Kang, S.-O. (1995) Role of laccase in lignin degradation by white-rot fungi, *FEMS Microbiol. Lett. 132*, 183-188.

30. Eggert, C., Temp, U., and Eriksson, K.-E. L. (1997) Laccase is essential for lignin degradation by the white-rot fungus *Pycnoporus cinnabarinus*, *FEBS Lett. 407*, 89-92.

31. Skalova, T., Dohnalek, J., Ostergaard, L. H., Ostergaard, P. R., Kolenko, P., Duskova, J., Stepankova, A., and Hasek, J. (2009) The Structure of the Small Laccase from *Streptomyces coelicolor* Reveals a Link between Laccases and Nitrite Reductases, *J. Mol. Biol. 385*, 1165-1178.

32. Bauer, S., Sorek, H., Mitchell, V. D., Ibanez, A. B., and Wemmer, D. E. (2012) Characterization of *Miscanthus giganteus* lignin isolated by ethanol organosolv process under reflux condition, *J. Agric. Food Chem. 60*, 8203-8212.

33. Kieser, T., Bibb, M. J., Buttner, M. J., Chater, K. F., and Hopwood, D. A. (2000) *Practical Streptomyces Genetics*.

34. Gust, B., Challis, G. L., Fowler, K., Kieser, T., and Chater, K. F. (2003) PCR-targeted *Streptomyces* gene replacement identifies a protein domain needed for biosynthesis of the sesquiterpene soil odor geosmin, *Proc. Natl. Acad. Sci. U S A 100*, 1541-1546.

35. Crawford, D. L., and Pometto, A. L., III. (1988) Acid-precipitable polymeric lignin: production and analysis, *Methods Enzymol. 161*, 35-47.

36. Motulsky, H., and Christopoulos, A. (2004) *Fitting Models to Biological Data using Linear and Nonlinear Regression. A Practicle Guide to Curve Fitting.*, Oxford University Press, New York.

37. Kabsch, W. (2010) Integration, scaling, space-group assignment and post-refinement, *Acta Crystallogr. D Biol. Crystallog.r 66*, 133-144.

38. Camarero, S., Ibarra, D., Martínez, Á. T., Romero, J., Gutiérrez, A., and del Río, J. C. (2007) Paper pulp delignification using laccase and natural mediators, *Enz. Microbia.l Technol. 40*, 1264-1271.

39. Diaz-Gonzalez, M., Vidal, T., and Tzanov, T. (2011) Phenolic compounds as enhancers in enzymatic and electrochemical oxidation of veratryl alcohol and lignins, *Appl. Microbiol. Biotechnol. 89*, 1693-1700.

40. Vallee, B. L., and Auld, D. S. (1993) Zinc: biological functions and coordination motifs, *Acc. Chem. Res. 26*, 543-551.

41. McCoy, A. J., Grosse-Kunstleve, R. W., Adams, P. D., Winn, M. D., Storoni, L. C., and Read, R. J. (2007) Phaser crystallographic software, *J. Appl. Crystallogr. 40*, 658-674.

42. Lamzin, V. S., and Wilson, K. S. (1997) Automated refinement for protein crystallography, *Methods Enzymol. 277*, 269-305.

43. Emsley, P., Lohkamp, B., Scott, W. G., and Cowtan, K. (2010) Features and development of Coot, *Acta Crystallographica, Section D: Biological Crystallography D66*, 486-501.

44. Adams, P. D., Afonine, P. V., Bunkoczi, G., Chen, V. B., Davis, I. W., Echols, N., Headd, J. J., Hung, L. W., Kapral, G. J., Grosse-Kunstleve, R. W., McCoy, A. J., Moriarty, N. W., Oeffner, R., Read, R. J., Richardson, D. C., Richardson, J. S., Terwilliger, T. C., and Zwart, P. H. (2010) PHENIX: a comprehensive Python-based

system for macromolecular structure solution, *Acta Crystallographica, Section D: Biological Crystallography D66*, 213-221.

45. Harwood, C. S., and Parales, R. E. (1996) The beta-ketoadipate pathway and the biology of self-identity, *Annu. Rev. Microbiol. 50*, 553-590.

46. Ahmad, M., Taylor, C. R., Pink, D., Burton, K., Eastwood, D., Bending, G. D., and Bugg, T. D. (2010) Development of novel assays for lignin degradation: comparative analysis of bacterial and fungal lignin degraders, *Mol. Biosyst. 6*, 815-821.

47. Lahtinen, M., Kruus, K., Boer, H., Kemell, M., Andberg, M., Viikari, L., and Sipila, J. (2009) The effect of lignin model compound structure on the rate of oxidation catalyzed by two different fungal laccases, *J. Mol. Catal. B Enzym. 57*, 204-210.

48. Jeffries, T. W. (1990) Biodegradation of lignin-carbohydrate complexes, *Biodegradation 1*, 163-176.

49. Arora, D. S., and Sharma, R. K. (2010) Ligninolytic fungal laccases and their biotechnological applications, *Appl. Biochem. Biotechnol. 160*, 1760-1788.

50. Dube, E., Shareck, F., Hurtubise, Y., Beauregard, M., and Daneault, C. (2008) Decolorization of recalcitrant dyes with a laccase from *Streptomyces coelicolor* under alkaline conditions, *J. Ind. Microbiol. Biotechnol. 35*, 1123-1129.

51. Leonowicz, A., Cho, N. S., Luterek, J., Wilkolazka, A., Wojtas-Wasilewska, M., Matuszewska, A., Hofrichter, M., Wesenberg, D., and Rogalski, J. (2001) Fungal laccase: properties and activity on lignin, *J. Basic. Microbiol. 41*, 185-227.

52. Li, K., Xu, F., and Eriksson, K. E. (1999) Comparison of fungal laccases and redox mediators in oxidation of a nonphenolic lignin model compound, *Appl. Environ. Microbiol. 65*, 2654-2660.

53. Andreu, G., and Vidal, T. (2011) Effects of laccase-natural mediator systems on kenaf pulp, *Bioresour. Technol. 102*, 5932-5937.

54. Mitchell, V., Taylor, C., and Bauer, S. (2013) Comprehensive Analysis of Monomeric Phenolics in Dilute Acid Plant Hydrolysates, *Bioenerg. Res.*, 1-16.

55. Hammel, K. E., Jensen, K. A., Jr., Mozuch, M. D., Landucci, L. L., Tien, M., and Pease, E. A. (1993) Ligninolysis by a purified lignin peroxidase, *J. Biol. Chem. 268*, 12274-12281.

56. Marzullo, L., Cannio, R., Giardina, P., Santini, M. T., and Sannia, G. (1995) Veratryl alcohol oxidase from Pleurotus ostreatus participates in lignin biodegradation and prevents polymerization of laccase-oxidized substrates, *J. Biol. Chem. 270*, 3823-3827.

57. Lyashenko, A. V., Zhukova, Y. N., Zhukhlistova, N. E., Zaitsev, V. N., Stepanova, E. V., Kachalova, G. S., Koroleva, O. V., Voelter, W., Betzel, C., Tishkov, V. I., Bento, I., Gabdulkhakov, A. G., Morgunova, E. Y., Lindley, P. F., and Mikhailov, A. M. (2006) Three-dimensional structure of laccase from *Coriolus zonatus* at 2.6 Å resolution, *Crystallogr. Rep. 51*, 817-823.

58. Polyakov, K. M., Fedorova, T. V., Stepanova, E. V., Cherkashin, E. A., Kurzeev, S. A., Strokopytov, B. V., Lamzin, V. S., and Koroleva, O. V. (2009) Structure of native laccase from *Trametes hirsuta* at 1.8 Å resolution, *Acta Crystallogr., Sect. D Biol. Crystallogr. D65*, 611-617.

59. Ge, H., Gao, Y., Hong, Y., Zhang, M., Xiao, Y., Teng, M., and Niu, L. (2010) Structure of native laccase B from *Trametes sp.* AH28-2, *Acta Crystallogr., Sect. F Struct. Biol. Cryst. Commun. F66*, 254-258.

60. Bonomo, R. P., Cennamo, G., Purrello, R., Santoro, A. M., and Zappala, R. (2001) Comparison of three fungal laccases from *Rigidoporus lignosus* and *Pleurotus ostreatus*: correlation between conformation changes and catalytic activity, *J. Inorg. Biochem. 83*, 67-75.

61. Enguita, F. J., Martins, L. O., Henriques, A. O., and Carrondo, M. A. (2003) Crystal structure of a bacterial endospore coat component. A laccase with enhanced thermostability properties, *J. Biol. Chem. 278*, 19416-19425.

62. Bento, I., Martins, L. O., Gato Lopes, G., Armenia Carrondo, M., and Lindley, P. F. (2005) Dioxygen reduction by multi-copper oxidases; a structural perspective, *Dal. Transac.*, 3507-3513.

63. Durao, P., Bento, I., Fernandes, A. T., Melo, E. P., Lindley, P. F., and Martins, L. O. (2006) Perturbations of the T1 copper site in the CotA laccase from *Bacillus subtilis*: structural, biochemical, enzymatic and stability studies, *J. Biol. Inorg. Chem. 11*, 514-526.

64. Kallio, J. P., Auer, S., Janis, J., Andberg, M., Kruus, K., Rouvinen, J., Koivula, A., and Hakulinen, N. (2009) Structure-function studies of a *Melanocarpus albomyces* laccase suggest a pathway for oxidation of phenolic compounds, *J. Mol. Biol. 392*, 895-909.

Table 1. APPL production by wild type *Streptomyces coelicolor* A3(2) (SCWT) and its laccase deficient mutant (SCΔLAC).

Culture	APPL production (mg) in cultures	
	SCWT	SCΔLAC
1	155	103.5
2	161.4	108.5
3	160.6	107

Table 2. Compositional analysis of APPL

Compound	SCWT [mg]	SCΔLAC [mg]
Glucan	6.87 ± 0.20	5.13 ± 0.10
Xylan	6.74 ± 0.06	4.25 ± 0.02
Arabinan	2.28 ± 0.07	2.51 ± 0.03
Acetyl	1.58 ± 0.06	0.67 ± 0.03
Klason lignin	155 ± 6	68.6 ± 4.0
Ash	83.1 ± 0.6	80.7 ± 0.7
Nitrogen	32.43	30.89

Table 3. Steady-state kinetic parameters for the laccases with LM-OH at pH 8.0.

Enzyme	k_{rel} (min^{-1})	K_{app} (mM)	k_{rel}/K_{app} ($min^{-1}mM^{-1}$)
SCLAC	26 ± 2	102 ± 14	25 ± 1 x 10^{-2}
SLLAC	29 ± 3	120 ± 17	24 ± 2 x 10^{-2}
SVLAC	39 ± 2	143 ± 10	27 ± 2 x 10^{-2}
AMLAC	10 ± 1	133 ± 7	8 ± 1 x 10^{-2}

Table 4. Data collection and refinement statistics for AMLAC.

	AMLAC•Cu^{2+}•LM-OMe	AMLAC•Cu^{2+}
Data collection		
Space group	$C222_1$	R32
No. of mol. in asym. Unit	3	1
Cell dimensions		
a, *b*, *c* (Å)	84.42, 115.26, 163.51	110.180, 110.180, 178.820
a, b, g (°)	90.00, 90.00, 90.00	90.00, 90.00,120.00
Resolution (Å)	19.80-2.35 (2.41-2.35)	19.85-1.50 (1.54-1.50)
No. of unique reflections	33545	66783
R_{merge}	0.101 (0.641)	0.078 (0.619)
I / sI	20.65 (2.71)	18.46 (2.6)
Completeness (%)	99.8 (99.8)	99.9 (100.0)
Refinement		
Resolution (Å)	19.80-2.35	19.66-1.50
R_{cryst}	0.176	0.172
R_{free}	0.238	0.202
R.m.s. deviations		
Bond lengths (Å)	0.008	0.008
Bond angles (°)	1.408	1.389
No. atoms		
Protein	6455	2192
Waters	264	468
Substrate	24	----

Metal ions	15	5
B-factors		
Wilson plot	29.8	18.0
Protein	29.7	20.1
Ligands	39.3	27.5
Solvent	27.8	35.4
PDB entry	3TA4	3T9W

Table 5. Data collection and refinement statistics for SVLAC.

	SVLAC•Cu^{2+}•Zn^{2+}	SVLAC•Cu^{2+}	SVLAC•Cu^{2+}•AV
Data collection			
Space group	I222	$P3_121$	$P3_121$
No. of mol. in asym. unit	3	3	3
Cell dimensions			
a, *b*, *c* (Å)	102.30, 157.18, 162.33	127.00, 127.00, 155.07	127.02, 127.02, 155.54
a, b, g (°)	90.00, 90.00, 90.00	90.00, 90.00, 120.00	90.00, 90.00, 120.00
Resolution (Å)	19.69-2.30 (2.36-2.30)	29.93-2.3 (2.38-2.30)	19.76-2.7 (2.77-2.70)
No. of unique reflections	58241	64657	40270
R_{merge}	0.20 (0.797)	0.164 (0.786)	0.157 (0.861)
I / sI	10.51 (2.02)	15.12 (2.23)	15.42 (2.20)
Completeness (%)	99.8 (99.9)	99.9 (100.0)	99.6 (99.9)
Refinement			

Resolution (Å)	19.69-2.30	29.93-2.3	19.76-2.70
R_{cryst}	0.147	0.161	0.157
R_{free}	0.193	0.206	0.210
R.m.s. deviations			
Bond lengths (Å)	0.008	0.008	0.008
Bond angles (°)	1.269	1.342	1.275
No. atoms			
Protein	6918	6450	6428
Waters	615	563	313
Substrate	----	----	12
Metal ions	18	12	12
B-factors			
Wilson plot	21.0	32.6	43.9
Protein	22.1	31.9	46.7
Ligands	20.6	39.4	64.3
Solvent	29.9	36.8	41.9
PDB entry	3TBB	3TAS	3TBC

LEGENDS TO FIGURES AND SCHEME

Figure 1. Results of APPL experiments. Panel A, medium alone. Panel B, medium with lignocellulose. Panel C, medium with wild type *Streptomyces coelicolor* A3(2) (SCWT). Panel D, medium with laccase deficient mutant (SCΔLAC). Panel E, medium with both lignocellulose and SCWT. Panel F, medium with both lignocellulose and SCΔLAC.

Figure 2. Oxidation of non-phenolic *β-O-4* lignin model compound (LM-OMe) in presence of laccase and mediator to the corresponding ketone derivative.

Figure 3. Reverse phase chromatography of the soluble fraction of ethanosolv lignin. The black line indicates the starting material; the red line indicates ethanosolv lignin reacted with SCLAC for 16 hr at 37 ˚C.

Figure 4. Size-exclusion chromatography of ethanosolv lignin. The mobile phase was 30% CH_3CN/H_2O. Black trace is unreacted ethanosolv lignin. Red trace is ethanosolv lignin that was reacted with SCLAC at 37 ˚C for 16h.

Figure 5. a) Two trimers related by crystallographic symmetry create a "wedge" in the AMLAC structure, which enables ligand binding on one side of the trimer-trimer interface; b) Stereo view of the ligand binding; electron density for the ligand molecule is contoured at 2.5σ on a difference (F_o-F_c) omit map; T1 designates the mononuclear copper center.

Figure 6. Stereo view of the binding geometry of acetovanillone in the SVLAC is shown. Electron density for acetovanillone is shown on a difference (F_o-F_c) omit map contoured at 3σ; the unoccupied density belongs to the symmetry related molecule of acetovanillone, which is not shown here. T1 denotes the mononuclear copper center.

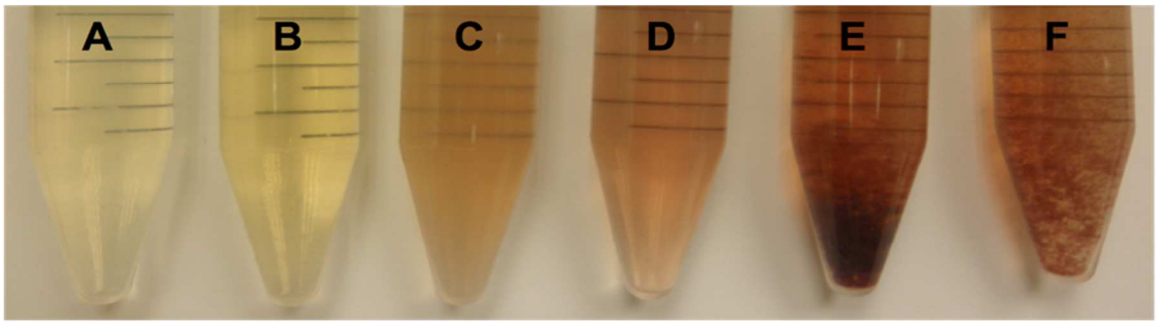

Figure 1, Majumdar *et al.*

Figure 2, Majumdar *et al*.

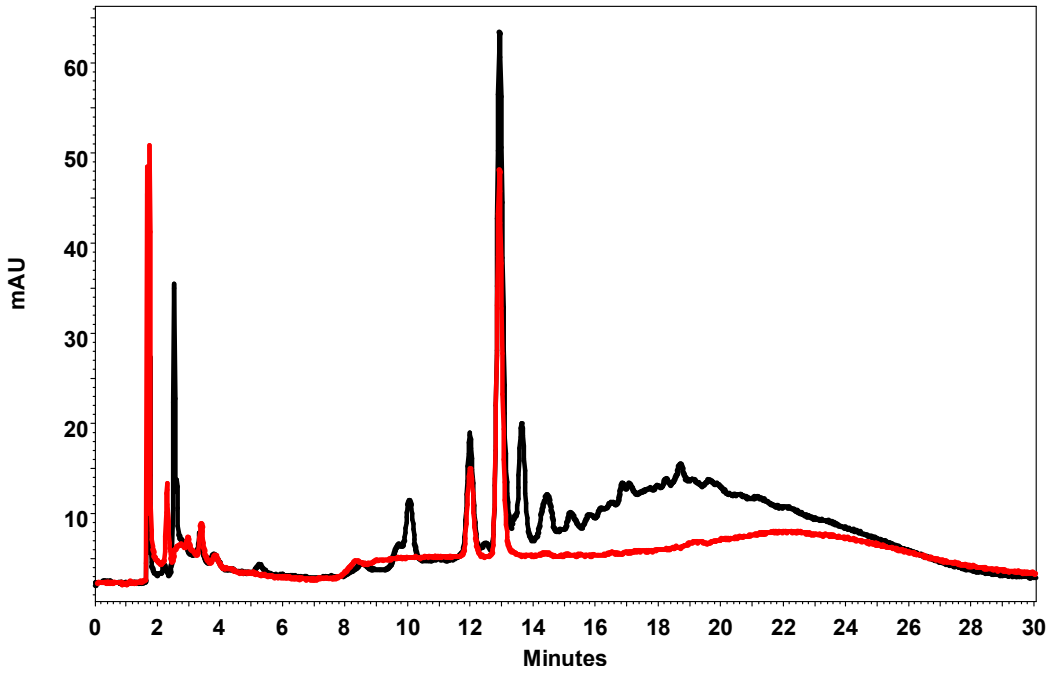

Figure 3, Majumdar *et al*.

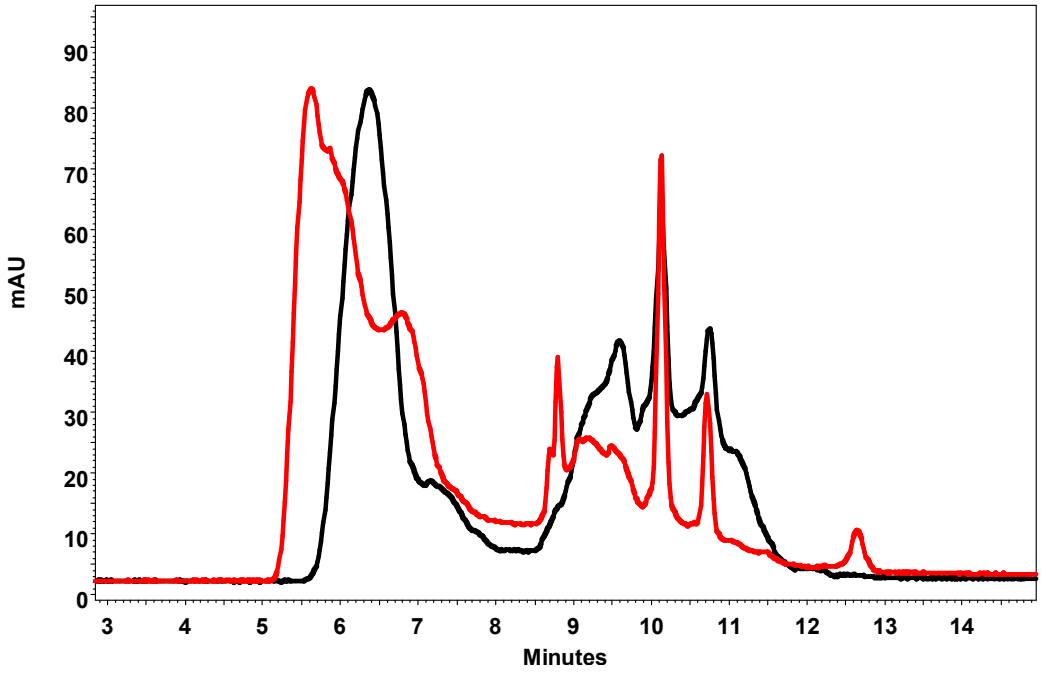

Figure 4, Majumdar *et al*.

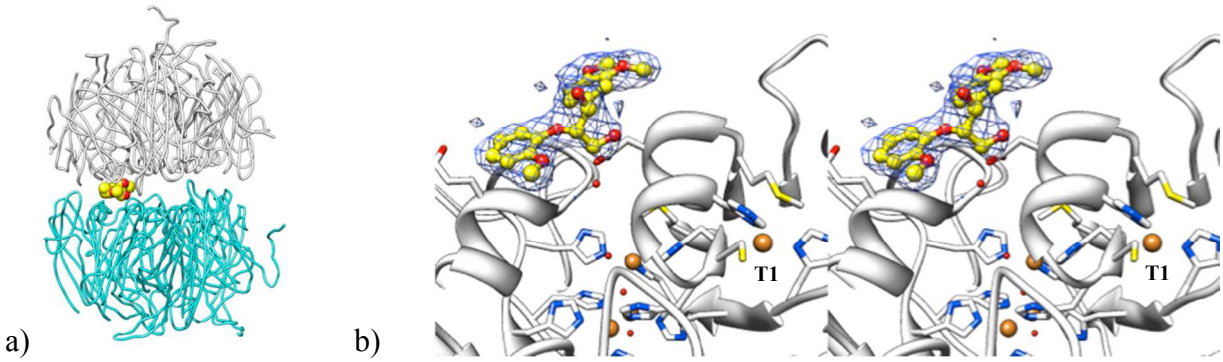

Figure 5, Majumdar *et al*.

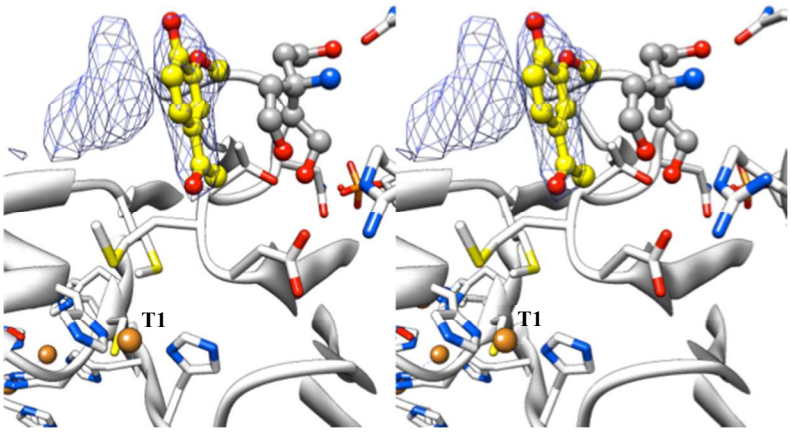

Figure 6, Majumdar *et al*.

Table of contents graphic:

The roles of small laccases from *Streptomyces* in lignin degradation

Sudipta Majumdar, Tiit Lukk, Jose O. Solbiati, Stefan Bauer, Satish K. Nair, John E. Cronan, and John A. Gerlt